TRAIL treatment prevents renal morphological changes and TGF-β-induced mesenchymal transition associated with diabetic nephropathy

Barbara Toffoli[1,*], Federica Tonon[2,*], Veronica Tisato[3], Andrea Michelli[2], Giorgio Zauli[3], Paola Secchiero[3], Bruno Fabris[2] and Stella Bernardi[2]

[1]Institute for Maternal and Child Health, IRCCS 'Burlo Garofolo', Via dell'Istria 65, Trieste 34100, Italy; [2]Department of Medical, Surgical and Health Sciences, University of Trieste, Cattinara Teaching Hospital, Strada di Fiume 447, Trieste 34100, Italy; [3]Department of Morphology, Surgery and Experimental Medicine and LTTA Centre, University of Ferrara, Via Fossato di Mortara 66, Ferrara 44100, Italy

Correspondence: Stella Bernardi (stella.bernardi@asuits.sanita.fvg.it, shiningstella@gmail.com)

Background: TNF-related apoptosis-inducing ligand (TRAIL) has attracted attention not only as an anti-cancer agent, but also as a potential treatment for diabetes. Animal studies have shown that TRAIL delivery ameliorated glucose control in type 1 and type 2 diabetes. It is currently unknown whether TRAIL positive effects are maintained in more severe forms of type 2 diabetes, and whether they include renoprotection. Our study aimed at evaluating TRAIL effects in a severe form of type 2 diabetes with nephropathy.
Materials and methods: A total of 20 db/db mice were treated with saline or TRAIL twice per week for 12 weeks. In parallel, renal tubular epithelial cells were cultured with TGF-β1 in the presence and absence of TRAIL, with and without silencing TRAIL-specific receptor (DR5) and leptin receptor.
Results: TRAIL did not improve glucose control, but it significantly reduced circulating interleukin (IL)-6 and resistin. In the kidney, TRAIL treatment significantly ameliorated glomerular and tubular morphology with an improvement in kidney function, but no effect on proteinuria. Our *in vitro* studies on TGF-β1-treated cells, showed that by binding to DR5, TRAIL rescued normal tubular cell morphology, increasing E-cadherin and reducing α-smooth muscle actin (SMA) expression, with no effects on cell viability. Interestingly, both *in vivo* and *in vitro*, TRAIL reduced the accumulation of the autophagy substrate p62.
Conclusions: Our data confirm TRAIL protective effects against organ damage and shed light on to promising anti-fibrotic actions, which are independent of glucose control. TRAIL anti-fibrotic actions might be due to the rescue of autophagy in diabetes.

Introduction

TNF-related apoptosis-inducing ligand (TRAIL) is a type II transmembrane protein that can be cleaved to form a circulating ligand, which belongs to the TNF family of apoptosis-inducing ligands. Both membrane-bound and circulating TRAIL are able to induce apoptosis of transformed cell lines but not of normal cells by binding to the specific receptors, TRAIL-R1 (DR4) and TRAIL-R2 (DR5) [1,2]. During the last two decades, TRAIL and its specific receptors have attracted attention as a pathway to target for cancer therapy [3,4].

A few recent studies suggest that TRAIL might protect not only against tumor development and progression, but also against non-neoplastic conditions, such as diabetes mellitus and its associated diseases. In particular, animal studies have shown that TRAIL deficiency was associated with the development of

*These authors contributed equally to this work.

Accepted: 28 August 2020

heightened autoimmune responses and worsening of type 1 diabetes [5,6], while TRAIL delivery attenuated disease severity, with partial preservation of islets morphology in streptozotocin-diabetic mice [7]. Likewise, we have recently documented that TRAIL delivery significantly attenuated the metabolic abnormalities induced by a high-fat diet [8,9], while TRAIL deficiency was found associated with worsening of glucose control in type 2 diabetes [10].

Although these studies have shown that TRAIL treatment was able to attenuate early forms of type 2 diabetes, such as the one induced by a high-fat diet, it is currently unknown what would be the effect of TRAIL treatment on a more severe form of type 2 diabetes. In addition, the effects of TRAIL on the diabetic kidney have not been clarified yet [11].

Based on this background, the aim of the present study was to evaluate TRAIL effects on a severe form of type 2 diabetes associated with diabetic nephropathy. For this reason, TRAIL effects were tested on the db/db mouse, which is one of the most widely used genetic models for the study of type 2 diabetes and diabetic nephropathy [12]. In particular, the *db* gene encodes for a G-to-T point mutation of the leptin receptor, leading to a defect in leptin signaling [13]. Lack of leptin signaling causes persistent hyperphagia and obesity, with subsequent insulin resistance and hyperglycemia. Overt hyperglycemia appears by the 6–10th week of age, peaking by the 14–16th week of age, when db/db mice become dependent on insulin to control their increasing glucose levels to survive. Albuminuria increases by 8- to 62-fold at the age of 8 weeks, and remain persistently elevated regardless of glucose control. Renal structural changes become evident after 16 weeks of age, including glomerular enlargement, mesangial matrix expansion and a marked increase in fibronectin and type IV collagen. Overall, given that db/db mice exhibit progressive glomerular changes in the setting of severe hyperglycemia, this is considered an appropriate mouse model for the study of diabetic nephropathy [14].

Materials and methods

Recombinant human TRAIL

Recombinant histidine-6-tagged human TRAIL (114-281) was produced in transforming bacteria BL21 with a pTrc-His6 TRAIL vector, as previously described [15].

Human TRAIL shares approximately 65% amino acid sequence homology with mouse TRAIL. It is active on mouse cells, without toxic effects, where it binds to DR5 [1,2], which is the only death receptor for TRAIL in mice. When injected into mice, human recombinant TRAIL is detectable for 6 h and then it decreases over time, disappearing by 24 h [9].

In vivo studies

Experimental protocol

A total of 15 db/H male mice (BKS.CG-M DB/+) and 20 db/db male mice (BKS.CG-M+/+LEPRDB/J, purchased from Charles River Laboratories) at 8 weeks of age were randomly allocated to saline (NaCl 0.9%) or TRAIL (rh-TRAIL) for 12 weeks. Mice were divided into the following four groups: db/H (db/H + saline, n=10); db/H + T (db/H + TRAIL, n=5); db/db (db/db + saline, n=10); db/db + T (db/db + TRAIL, n=10). TRAIL was given at the dose of 15 μg/200 μl twice per week for 12 weeks. Insulin was administered for the last 2 weeks of the study (after the intraperitonal insulin tolerance test (IPITT)).

Animals were kept in a pathogen-free environment at the Animal House of the Cluster in Biomedicine (CBM S.c.r.l. Area Science Park, Trieste, Italy). They were housed five per cage in ventilated cabinets (Tecniplast Spa) in a temperature-controlled room (22°C), with relative humidity of 50–70%, on a 12-h light/12-h dark cycle with free access to food and water. All the mice were fed with a standard diet, providing 22% of calories from protein, 66% of calories from carbohydrate and 12% of calories from fat, and a digestible energy of 3.0 kcal/g (Tekland Global 16% Protein Rodent Diet).

During the 12-week study period, body weight and food intake were measured every week, while glucose, insulin and albuminuria were measured every 4 weeks. Tolerance tests were performed at the end of the study. At the end of the study, animals were anesthetized by an IP injection of tiletamine/zolazepam (80 mg/kg). Blood was collected from the left ventricle, centrifuged and serum was stored for further analyses.

All the experimental procedures were performed in strict accordance with the recommendations of the Guide for the Care and Use of the Laboratory Animals of the National Institutes of Health and in compliance with the European (86/609/EEC) and Italian (D.L.116/92) laws. The present study was approved by the Institutional Animal Care and Use Committee of the Cluster in Biomedicine (CBM) and by the Italian Ministry of Health (DM 17/2001 – 712/2016-PR). The study period was from January 2017 to July 2019.

General parameters and biochemistries

Food intake was measured by placing the pellets in the cages previously weighed in total. The food left over was collected and weighed to find the amount eaten. Fasting glucose was measured by glucometer (GlucoMen LX Plus, Menarini). Fasting insulin was measured by ELISA (#EZRMI-13K; Millipore). Urinary albumin/creatinine ratio (ACR) was evaluated on spot urines [16] with Albuwell M ELISA kit (#1011 Exocell) coupled with the Creatinine Companion kit (#1012 Exocell). Creatinine and plasma urea nitrogen were measured by autoanalyzer (Beckman Coulter). Leptin, resistin, interleukin (IL)-6 and monocyte chemoattractant protein (MCP)-1 were measured with a multiplex assay (#MADCYMAG-72K, Millipore).

Tolerance tests

The intraperitoneal insulin tolerance test (IPITT) was performed on day 1 of week 11 by injecting insulin (1 unit/kg) intraperitoneally after a 6-h fast and measuring glucose by glucometer at baseline, 30, 60 and 120 min. The intraperitonal glucose tolerance test (IPGTT) was performed on day 1 of week 12 by injecting glucose (1 g/kg) intraperitoneally after an overnight fast and then measuring glucose and collecting blood at baseline and at 15, 60 and 120 min. Blood samples were then centrifuged to collect the sera, where insulin was measured.

In vitro studies

Induction of epithelial-to-mesenchymal transition on NRK-52E cells

Normal rat kidney tubular epithelial cells (NRK-52E) were purchased from Sigma–Aldrich. Cells were maintained in DMEM that contained 25 mM glucose with 5% new born calf serum (NBCS), penicillin (100 μg/ml), streptomycin (100 mg/ml) and L-glutamine (2 mM; Gibco BRL), in a 5% CO_2 atmosphere and they were passaged twice a week. In order to induce epithelial-to-mesenchymal transition (EMT) [17], cells were seeded at a density of $5.5 \times 10^3/cm^2$ and treated twice with either TGF-β1 (10 ng/ml, R&D Systems), or vehicle, with or without TRAIL (1 ng/ml) for 6 days. In order to evaluate cell viability and their size, cells were cultured in 96-well plates and assessed with the MTT assay according to manufacturer's instructions (Merck) and the Countess™ II Automated Cell Counter (Thermo Fisher Scientific), respectively. Then, in order to evaluate TRAIL effects on TGF-β1-induced EMT, cells were cultured in 6- or 12-well plates for 6 days (with a medium change). Morphologic changes were evaluated under a light microscope before harvesting for mRNA or fixing for immunofluorescence.

DR5 and *Lepr* siRNA transfection

In order to evaluate if TRAIL effects were mediated by DR5 and blunted in the absence of LEPR, siRNA sequences directed to two different regions of the *Dr5* and *Lepr* gene were purchased from Life Technologies. For transfection, NRK-52E cells were seeded at a density of $5 \times 10^3/cm^2$ in 6- or 12-well plates and allowed to recover for 24 h. Then, they were transfected with 100 nM of *Dr5*, *Lepr* and CTR siRNA (Life Technologies) using RNAiMAX (Life Technologies) for 5 h.

Stainings

Renal histomorphology

Four-micrometer-kidney sections were stained with Hematoxylin and Eosin (H/E) and with Periodic acid–Schiff (PAS) reagent. Glomerular cross-sectional area was calculated by tracing the outline of the glomerular tuft [18]. The glomerulosclerosis index was scored on 50 glomeruli from each section with a range from 0 to 4 (0 is for no change; 1 is for changes affecting <25%; 2 is for changes affecting 25–50%; 3 is for changes affecting 50–75%; 4 is for changes affecting >75% of the glomerulus) [19].

Renal immunostaining

For immunohistochemical staining, 4-μm-paraffin kidney sections were incubated overnight at 4°C with the following primary antibodies: rabbit anti-collagen IV (1:400, #2150–1470, Bio-Rad), rabbit anti-nitrotyrosine (1:100, #06-284, Millipore), rabbit anti-TRAIL (1:400, #GTX11700, GeneTex) and rabbit anti-DR5 (1:500, #LS-B136/142896, LifeSpan Biosciences). Then, all sections were incubated with goat anti-rabbit biotinylated secondary antibodies (Vector Laboratories), followed by the standard avidin–biotin complex (Vector Laboratories) method. The final detection step was carried out using 3,3′-diaminobenzidine tetrahydrochloride (DAB; Sigma Chemical), and after counterstaining with Hematoxylin, all the sections were examined by light microscopy (Carl Zeiss-Jenaval) and digitized with a high-resolution camera (Q-Imaging Fast 1394). The percentage of stained area was evaluated in 50 glomeruli from each section using Image-Pro Plus 6.3 (Media Cybernetics). For immunofluorescence staining, 4-μm-paraffin kidney sections were subjected to antigen retrieval with citrate buffer (pH 6) before incubation with primary antibody

anti-synaptopodyn (1:10, #61094, Progen) overnight at 4°C. All sections were incubated with goat anti-mouse (1:300, Alexa Fluor 488, Invitrogen) for 30 min. Images were captured on a Leica DM-2000 microscope (Leica Microsystems), and they were quantified with Image-Pro Plus 6.3 (Media Cybernetics).

NRK-52 immunostaining

To detect E-Cadherin, NRK-52E cells were fixed with 4% paraformaldehyde for 20 min at room temperature. After permeabilization and rehydration with 0.1% Triton-X 100 for 5 min and 1.5% BSA/PBS for 30 min, they were incubated with a rabbit anti-E-Cadherin antibody (1:100, #PA5-85088, Invitrogen) overnight at 4°C and then with a fluorescent goat anti-rabbit antibody (1:300, Alexa Fluor 568, Invitrogen) for 45 min at room temperature. To detect α-smooth muscle actin (SMA), cells were fixed with ice-cold acetone for 20 min at −20°C. After permeabilization and rehydration, cells were incubated with a mouse anti-α-SMA antibody (1:250, #M0851, Dako) for 1 h, and then with the secondary goat anti-mouse (1:300, Alexa Fluor 488, Invitrogen) for 45 min at room temperature. Images were captured on a Leica DM-2000 microscope (Leica Microsystems), and they were quantified with Image-Pro Plus 6.3 (Media Cybernetics).

Gene expression quantification by real-time RT-PCR

In vivo study

Renal tissue was homogenized with 1 ml of Trizol (Invitrogen) per 100 mg of tissue. In order to isolate mRNA, 200 µl of chloroform/isoamyl alcohol were added to each tube and the samples were vortexed for 15 s and left at room temperature for 5 min. Then samples were centrifuged at 13000 rpm for 20 min and the upper aqueous phase was carefully removed to new tubes. In order to precipitate RNA, 500 µl of isopropanol were added to each tube, the tubes briefly vortexed and left at −20°C overnight. The day after, samples were centrifuged at 13000 rpm for 15 min at 4°C to pellet the RNA precipitate. The supernatant was then carefully discarded by inversion and 1 ml of 75% ethanol was added per tube and the tubes left at room temperature and then centrifuged for 15 min at 13000 rpm. The supernatant was entirely removed, the RNA was resuspended in 45 µl of RNAse-free water and incubated at 55°C for 5 min, before quantifying RNA. RNA was treated with DNAse to eliminate DNA contamination (#AM-1906, Ambion DNA-free product), and 3 µg of treated RNA were subsequently used to synthesize cDNA with Superscript First-Strand synthesis system for RT-PCR (Gibco BRL). The gene expression of *Col1a1*, *Col3a1*, *Ccn2* (*CTGF*), *Fn1* (*fibronectin*), *Mmp9*, *Tgf*β, *Vim* (*vimentin*), *Il-1*β, *Il-6*, *Ccl2* (*MCP1*), *Bax/Bcl2*, *Cdkn1a* (*P21*), *Tnfsf10* (*Trail*), *Tnfrsf10b* (*Dr5*), *Atg7*, *Atg5* and *Becn1* was analyzed by real-time quantitative RT-PCR using the SYBR Green system. The fluorescence for each cycle was analyzed quantitatively by StepOnePlus real-time PCR system (Applied Biosystems). Gene expression of the target sequence was normalized in relation to the expression of an endogenous control, *Rps9*.

In vitro study

RNA was extracted, processed and treated as it was specified before. Gene expression of *Tnfrsf10b* (*Dr5*), *Lepr*, *Acta2* (*α-SMA)*, *Col1a* (*Collagen Type I*), *Col4a* (*Collagen Type IV*) were analyzed by RT-PCR using the SYBR Green System (Life Technologies). Gene expression of *Fn1* (*fibronectin*), *CTGF*, *TGF-*β, *Nos2* (*iNos*) and *Nox4* was analyzed by RT-PCR using the TaqMan system (Life Technologies). The fluorescence for each cycle was analyzed quantitatively by StepOnePlus real-time PCR system (Applied Biosystems). Gene expression of the target sequence was normalized to *Gapdh* or *18s*. Results are reported as a ratio compared with the level of expression in untreated controls, which were given an arbitrary value of 1. **Primers are reported in Supplementary Table S1.**

Western blot analyses

Proteins were extracted from whole-cell lysates or tissue with Ripa Lysis Buffer (Millipore), 40 µg of protein were separated on SDS/PAGE and then transferred on to nitrocellulose membranes (GE Healthcare; Life Sciences) by semidry transfer (Semi Dry Transfer Cell; Bio-Rad, Hercules, CA). Transfer quality was verified with Ponceau S staining (Sigma–Aldrich). After transfer, all incubations were conducted on a rocking platform. The membrane was blocked in 5% skim milk/PBS/0.1% Tween with anti-p62 (1:1000, #P0067, Sigma–Aldrich), with anti-DR5 (1:1000, #LS-B136/142896, LifeSpan Biosciences) or with anti-Vimentin (1:200, #sc-6260, Santa Cruz Biotechnology), and in 5% BSA/PBS/0.1% Tween with anti-GAPDH (1:5000, #2118, Cell Signaling Technology) and then incubated overnight at 4°C. After washing, membranes were incubated with goat anti-rabbit HRP (#sc-2004, Santa Cruz Biotechnology) or goat anti-mouse HRP (#sc-2005, Santa Cruz Biotechnology) for 1 h at room temperature. Immunoreactivity was detected using an enhanced chemiluminescence kit (Bio-Rad) and exposure to Chemidoc Imaging system (Bio-Rad).

Statistical analysis

All statistical analyses were performed with Prism 5.0 (GraphPad Software, La Jolla, California, U.S.A.) or R. Shapiro–Wilk test was applied to continuous variables to check for distribution normality. Values were expressed as mean ± SEM and/or dot plots (horizontal bars are medians) according to statistical distribution (or number of mice). In *in vivo* studies, two-way ANOVA was used to assess the statistical significance of genotype and treatment over time (P-value adjusted with Bonferroni method). Comparisons between two groups were performed with t test or Mann–Whitney test based on distribution/number of mice (Mann–Whitney test was used for groups <5 mice). In *in vitro* studies, t test, one-way or two-way ANOVA were used. A P-value <0.05 was considered statistically significant.

Results

TRAIL treatment did not change body weight and metabolic abnormalities in db/db mice, but it reduced systemic inflammation

Due to the lack of leptin receptor, the db/db mouse model is characterized by the development of hyperphagia, obesity, insulin resistance and hyperglycemia. In our study, from the age of 8 weeks onward, db/db mice exhibited increased food intake and body weight as compared with their controls, which did not change after TRAIL treatment (Figure 1A,B). In addition, db/db mice exhibited hyperinsulinemia from the beginning of the study, while hyperglycemia appeared a few weeks later (Figure 1C,D). TRAIL did not modify such parameters. At the end of the study, db/db mice displayed significant hyperglycemia after an insulin and a glucose load, which did not change after TRAIL treatment (Figure 1E,F). In addition, db/db mice exhibited hyperleptinemia, which was lowered—although not significantly—by TRAIL treatment (Figure 1G). By contrast, TRAIL treatment significantly reduced circulating IL-6 and resistin (Figure 1H–J).

TRAIL treatment did not change albuminuria, but it reduced creatinine

When looking at the kidney, total kidney weights did not differ between the groups. Nevertheless, db/db mice exhibited lower kidney to body weight ratios, given their greater body weight. In particular, kidney/body weight was 7.01 ± 0.14 mg/g in db/H mice, 7.09 ± 0.2 in db/H + T mice, 4.43 ± 0.02 in db/db mice and 3.94 ± 0.19 in db/db + T mice. From the age of 8 weeks onward, db/db mice exhibited a significant and progressive increase in the urinary ACR (Figure 2A). TRAIL did not modify albuminuria in db/db mice (Figure 2A), it lowered plasma urea nitrogen in db/db mice—although not significantly (median value was 16.57 mmol/l in db/db mice and 13.92 mmol/l in db/db + TRAIL), while it significantly reduced creatinine (Figure 2B).

TRAIL treatment significantly ameliorated renal histomorphology, reducing kidney fibrosis

When looking at the kidney sections, db/db mice displayed glomerular hypertrophy, as assessed by H/E staining, and glomerulosclerosis, as assessed by PAS staining. TRAIL significantly decreased both (Figure 2C,D). In addition, db/db mice displayed tubular hypertrophy and the presence of a tubular inflammatory infiltrate, which were significantly reduced by TRAIL (Figure 2E,F). The renal expression of vimentin, as well as the glomerular expression of collagen IV and nitrotyrosine, which indicate the presence of fibrosis and oxidative stress, were all increased in db/db mice, and they were significantly reduced by TRAIL (Figure 3A–C). Interestingly, TRAIL treatment increased synaptopodin expression, which is a podocyte marker, as compared with db/db mice (Figure 3D). Consistent with these data, our gene expression analysis showed that several markers of fibrosis, such as *Col1a1*, *Fn1* (also known as *Fibronectin*) and *Vim* (*Vimentin*) significantly increased in the kidneys of db/db mice, and they were reduced by TRAIL treatment (Table 1). This also happened to proinflammatory cytokines, such as *IL-1*β and *IL-6*, whose gene expression significantly increased in db/db mice and was significantly reduced by TRAIL (Table 1).

TRAIL and DR5 renal expression

Gene expression analyses showed that *Tnfsf10* (*Trail*) and *Tnfrsf10b* (*Dr5*) were down-regulated in the kidneys of db/db mice as compared with db/H (Table 1). These changes were not affected by TRAIL treatment (Table 1). To confirm these results, kidney sections were immunostained for TRAIL and DR5 (Figure 3E,F). Semiquantitave analysis of TRAIL expression showed that TRAIL was significantly reduced in the glomeruli and tubuli of db/db mice as compared with db/H, while DR5 did not change (Figure 3E,F).

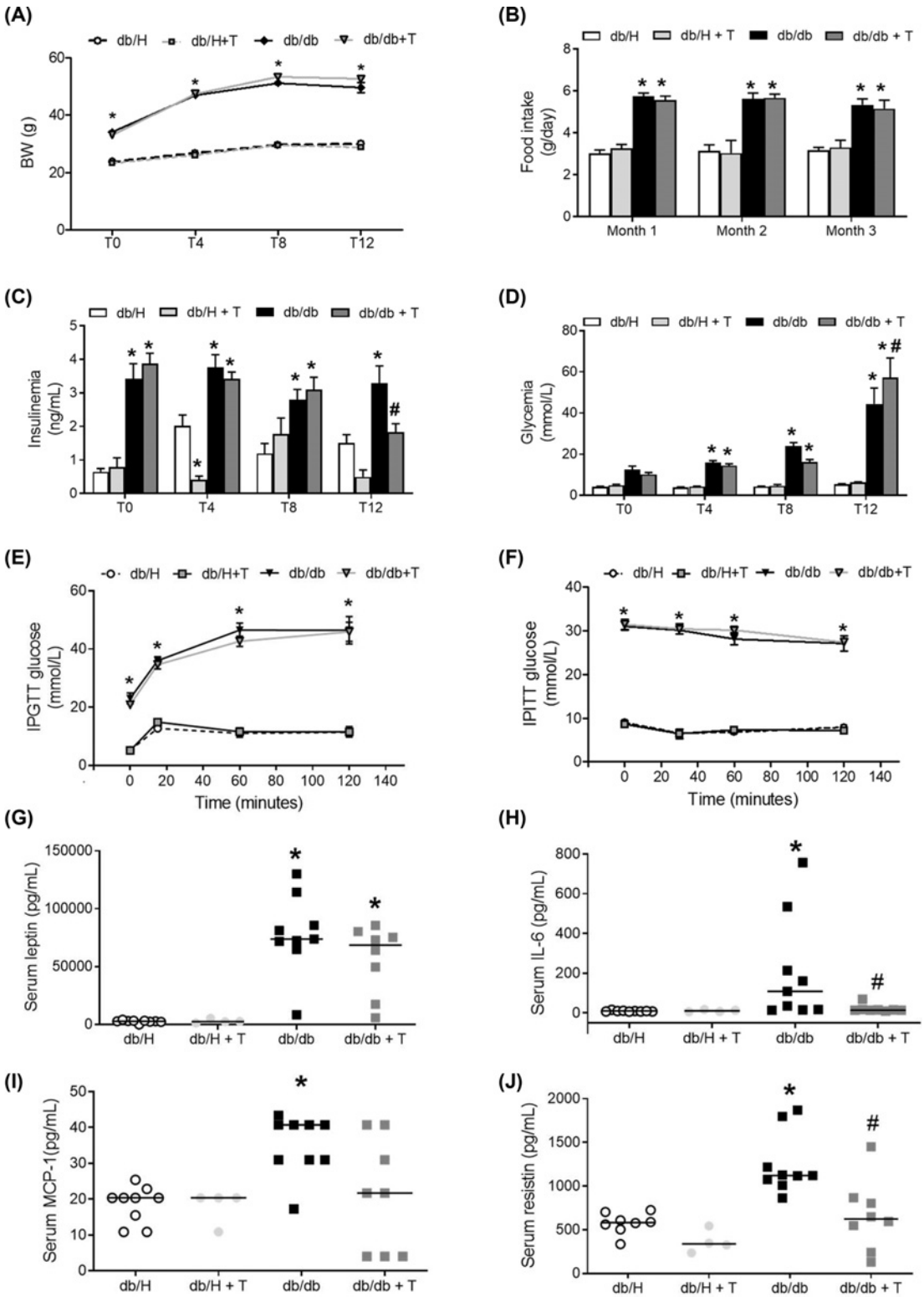

Figure 1. Body weight, food intake, glucose metabolism and inflammation

(**A**) Body weight and (**B**) food intake throughout the study. (**C**,**D**) Fasting insulin and glucose evaluated every 4 weeks (T0, T4, T8 and T12). (**E**) Blood glucose during an IPGTT. (**F**) Blood glucose during an IPITT. Results are presented as mean ± SEM; $^{*}P<0.05$ vs db/H; $^{\#}P<0.05$ vs db/db, two-way ANOVA. (**G**) Serum leptin (pg/ml), $^{*}P<0.001$ vs db/H. (**H**) Serum IL-6 (pg/ml), $^{*}P<0.001$ vs db/H and $^{\#}P=0.02$ vs db/db. (**I**) Serum MCP-1 (pg/ml), $^{*}P=0.002$ vs db/H. (**J**) Serum resistin (pg/ml), $^{*}P<0.001$ vs db/H and $^{\#}P<0.005$ vs db/db.

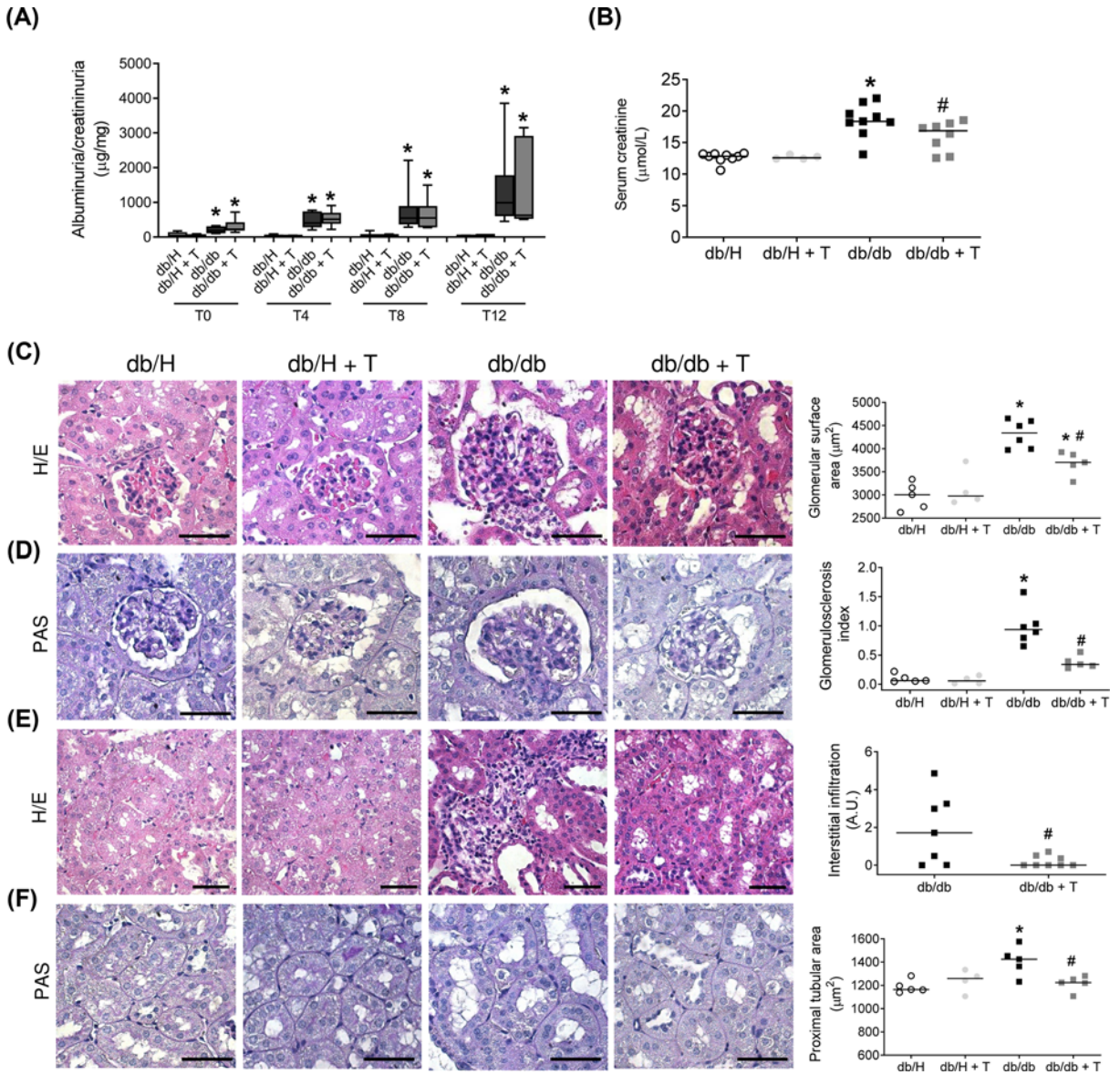

Figure 2. Renal functional and morphological changes

(**A**) Urine albumin/creatinine (μg/mg) ratio evaluated on spot urines during the study period. Data are expressed as box plots with the maximum and minimum values displayed with vertical lines; **P*<0.05 vs db/H, two-way ANOVA. (**B**) Serum creatinine (μmol/l); **P*<0.001 vs db/H and #*P*=0.02 vs db/db. (**C**) Representative images of glomeruli stained for H/E and evaluation of glomerular surface area (hypertrophy); **P*=0.014 vs db/H and #*P*=0.025 vs db/db. (**D**) Glomerular PAS staining and quantification of the glomerulosclerosis index; **P*=0.004 vs db/H; #*P*=0.004 vs db/db. (**E**) Representative images of renal tubules stained for H/E. db/db mice presented areas of inflammatory infiltration. Scatter dot plot shows interstitial inflammatory infiltration. #*P*=0.038 vs db/db. (**F**) Tubular PAS staining and quantification of the proximal tubular area. **P*=0.007 vs db/H; #*P*=0.019 vs db/db. In all the images the scale bar represents 50 μm.

TRAIL treatment prevented TGF-β-induced EMT of tubular cells

The effects of TRAIL were evaluated *in vitro*, on kidney tubular epithelial cells that were cultured with TGF-β1. TRAIL did not affect cell viability (Figure 4A). As assessed by both light microscopy and immunofluorescence, the untreated cells exhibited the typical cobblestone morphology of epithelial cells, with strong expression of E-cadherin and little expression of α-SMA. Treatment with TGF-β1 led to the induction of morphological changes, including elongation and hypertrophy (Figure 4B) and separation from neighboring cells (Figure 4C). Immunofluorescence

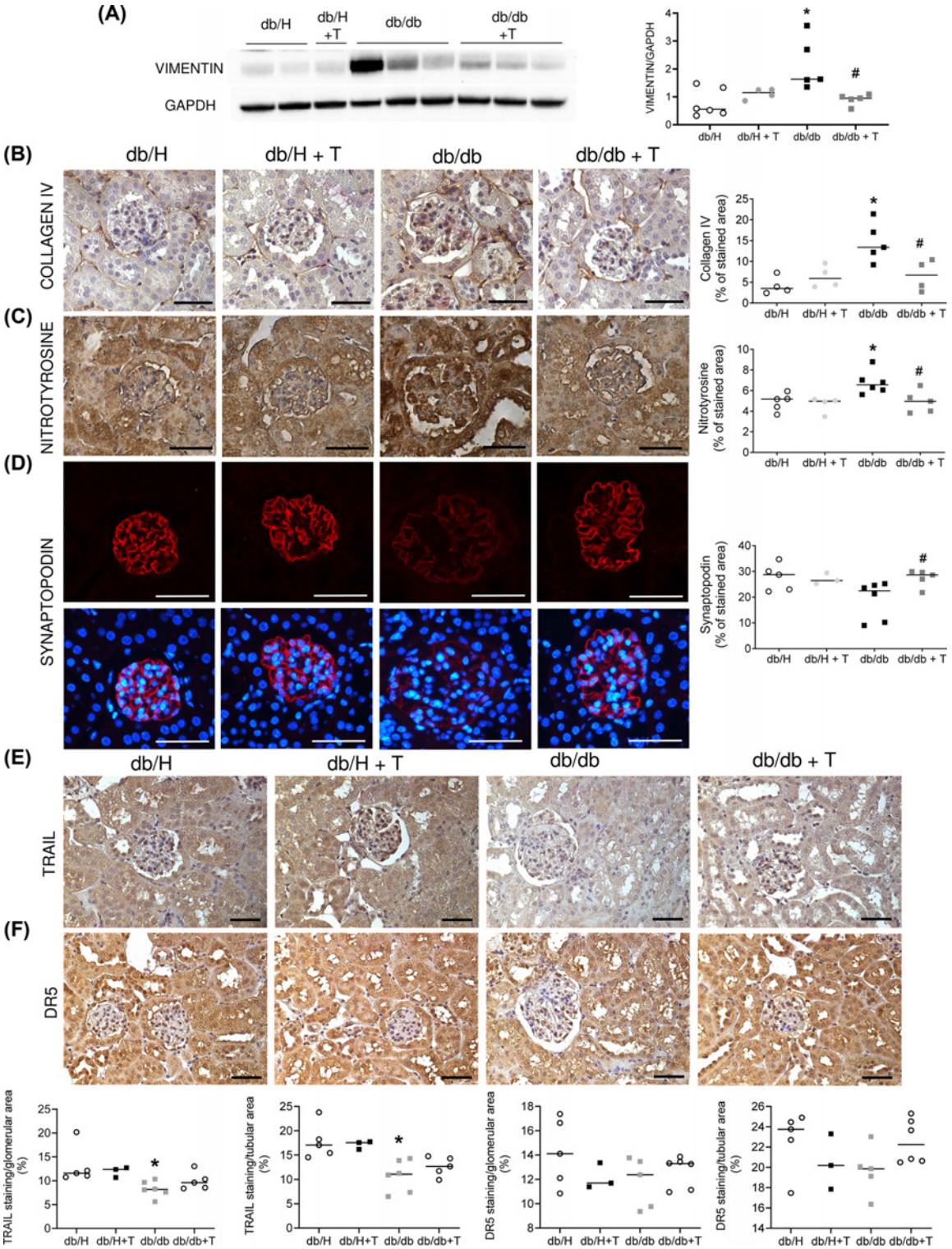

Figure 3. Renal Western blots and immunostainings

(**A**) Representative blot and densitometric analysis of vimentin in the kidney. Data are normalized to GAPDH. *P=0.013 vs db/H; #P=0.045 vs db/db. (**B**) Representative images of collagen IV and its quantification in the glomeruli. *P=0.005 vs db/H; #P=0.032 vs db/db. (**C**) Representative images of glomerular nitrotyrosine staining and its quantification in glomeruli. *P=0.037 vs db/H; #P=0.044 vs db/db. (**D**) Representative images of synaptopodyn staining. #P=0.030 vs db/db. (**E**) Representative images of TRAIL and its quantification in the glomeruli (*P=0.021 vs db/H) and tubuli (*P=0.005 vs db/H) (bottom left panels). (**F**) Representative images for DR5 and its quantification in the glomeruli and tubuli (bottom right panels). In all the images scale bar represents 50 μm.

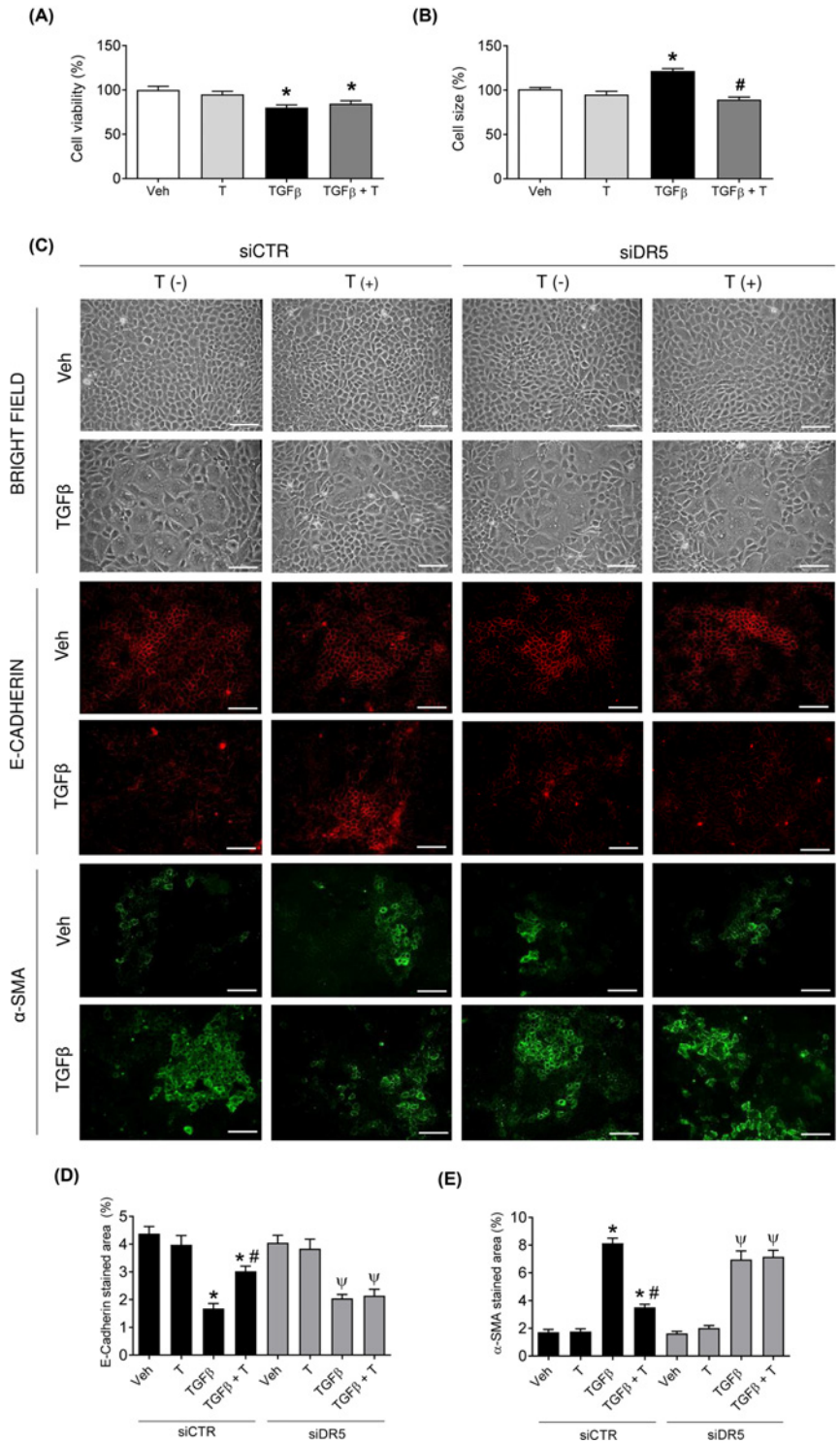

Figure 4. Effects of TRAIL treatment on TGF-β-induced EMT of tubular cells

(**A**) Cell viability as assessed by MTT assay and (**B**) cell size. Data are normalized to Veh (vehicle). Results are expressed as mean ± SEM. *$P<0.05$ vs Veh . (**C**) Representative images of NRK-52E cells after a 6-day treatment with TGF-β1 (10 ng/ml) and/or TRAIL (1 ng/ml) with or without *Dr5* silencing. Si-CTR indicates no silencing, while siDR5 indicates *Dr5* silencing. Bright field (top panels), E-cadherin immunofluorescence (red, middle panels), α-SMA immunofluorescence (green, bottom panels). Scale bar represents 100 μm. (**D**) Quantification of E-Cadherin positive red staining and (**E**) α-SMA positive green staining per area of NRK-52E fixed cells. Results were obtained by three independent experiments and are presented as mean ± SEM. *$P<0.05$ vs Veh and $^{\#}P<0.05$ vs TGFβ in the siCTR group. $^{\Psi}P<0.05$ vs Veh in the siDR5 group. Veh is for vehicle, T is for TRAIL.

Table 1 Renal gene expression

	db/H	db/H+T	db/db	db/db+T
Col1a1	1.04 (0.52–1.48)	1.04 (0.90–1.38)	5.18 (1.46–10.68)*	0.86 (0.56–3.31)†
Col3a1	0.99 (0.67–1.40)	0.78 (0.62–0.90)	1.04 (0.67–9.92)	0.60 (0.41–1.46)†
Ccn2 (*CTGF*)	1.10 (0.54–1.38)	0.94 (0.69–1.03)	1.32 (0.38–1.69)	1.06 (0.78–1.66)
Fn1 (fibronectin)	0.96 (0.76–1.45)	0.97 (0.61–1.05)	1.88 (1.21–4.74)*	1.11 (0.79–1.25)†
Mmp9	0.91 (0.74–1.66)	0.88 (0.61–1.60)	2.58 (0.59–4.08)	0.61 (0.52–1.08)†
Tgf-β	1.10 (0.67–1.24)	1.02 (0.92–1.10)	1.20 (0.91–2.48)	0.71 (0.49–1.02)†
Vim (vimentin)	1.00 (0.89–1.14)	1.03 (0.75–1.23)	1.60 (1.27–4.85)*	1.13 (0.81–1.32)†
Il-1β	0.81 (0.69–2.66)	1.25 (1.09–1.66)	14.68 (1.62–20.41)*	0.44 (0.25–4.79)†
Il-6	1.33 (0.37–2.09)	1.31 (0.69–4.66)	60.44 (1.40–92.81)*	0.60 (0.50–1.88)†
Ccl2 (MCP1)	0.92 (0.59–1.91)	0.80 (0.53–1.15)	1.21 (0.43–3.44)	0.48 (0.24–0.78)†
Bax/Bcl2	1.04 (0.83–1.19)	1.01 (0.97–1.27)	1.07 (0.98–9.43)	1.12 (1.03–1.32)
Cdkn1a (p21)	1.00 (0.67–1.63)	0.79 (0.64–0.89)	2.19 (1.51–7.44)*	1.74 (0.84–3.21)
Tnfrsf10b (Dr5)	1.03 (0.81–1.16)	1.00 (0.88–1.38)	0.66 (0.36–1.16)	0.53 (0.30–0.74)*
Tnfsf10 (Trail)	1.09 (0.65–1.24)	1.12 (0.74–1.23)	0.58 (0.48–0.85)*	0.48 (0.24–0.78)*
Atg7	1.16 (0.49–1.57)	1.32 (1.14–1.43)	1.23 (0.55–0.171)	1.25 (1.05–1.46)
Atg5	0.91 (0.62–1.41)	1.09 (0.64–1.38)	0.72 (0.45–0.96)	1.03 (0.93–1.18)†
Becn1	1.09 (0.56–1.47)	1.29 (1.23–1.31)	1.01 (0.32–1.36)	1.03 (0.66–1.26)

*$P<0.05$ vs db/H.
†$P<0.05$ vs db/db.

showed that TGF-β1 reduced E-Cadherin expression (Figure 4D), which is a marker of epithelial phenotype, and increased α-SMA expression (Figure 4E), which is a marker of the mesenchymal phenotype, indicating the induction of EMT. The addition of TRAIL to TGF-β1-treated cells significantly ameliorated these morphological changes, restoring cellular normal features and reducing EMT. In particular, TRAIL treatment significantly increased E-cadherin and reduced α-SMA expression in TGF-β1-treated cells, with no effects on untreated cells (Figure 4C–E).

TRAIL effects are mediated by binding to DR5

To evaluate whether TRAIL effects on tubular cells were mediated by its binding to DR5, cells were transfected with siRNA to *Dr5*. The efficiency of the siRNA knockdown was assessed by gene expression and Western blot analyses (Figure 5), indicating that DR5 was significantly reduced by siRNA transfection (40% reduction). Going back to bright field and immunofluorescence studies, the knockdown of *Dr5* significantly prevented TRAIL effects on the changes induced by TGF-β1, as the number of cells expressing E-Cadherin was reduced, while the number of cells expressing α-SMA increased (Figure 4C–E). In addition, TGF-β1 alone significantly increased the expression of pro-fibrotic *Col1a1, CTGF, Fn1* (*fibronectin*), *TGF-β* and pro-oxidative *Nos2* (*iNos)* and *Nox4* genes, which were all reduced by cotreatment with TRAIL (Figure 6). *Dr5* silencing prevented TRAIL effects on TGF-β1-induced gene expression (Figure 6).

The knockdown of leptin receptor does not affect TRAIL anti-fibrotic effects

To evaluate whether TRAIL effects on tubular cells could be impaired by the deletion mutation of the leptin receptor, which is the feature of db/db mice, tubular cells were transfected with siRNA to *Lepr*. In order to assess the efficiency of the siRNA knockdown, the gene expression of *Lepr* was quantified by real-time RT-PCR, and it was significantly reduced by siRNA transfection (Figure 7A). The knockdown of *Lepr* did not change TRAIL effects in terms of *Acta2* (*α-SMA*) expression (Figure 7B).

TRAIL treatment significantly reduces p62 levels in the kidney of db/db mice

Based on the observation that ATG5 was partially down-regulated in db/db mice and then restored by TRAIL treatment (Table 1), we hypothesized that TRAIL might restore autophagy in the diabetic kidney, where authophagy seems to be impaired [20]. For this reason, we quantified p62/SQSTM1, which is a substrate for authophagy degradation, which decreases during autophagy progression, whereas it increases with the inhibition of autophagy. In the kidney

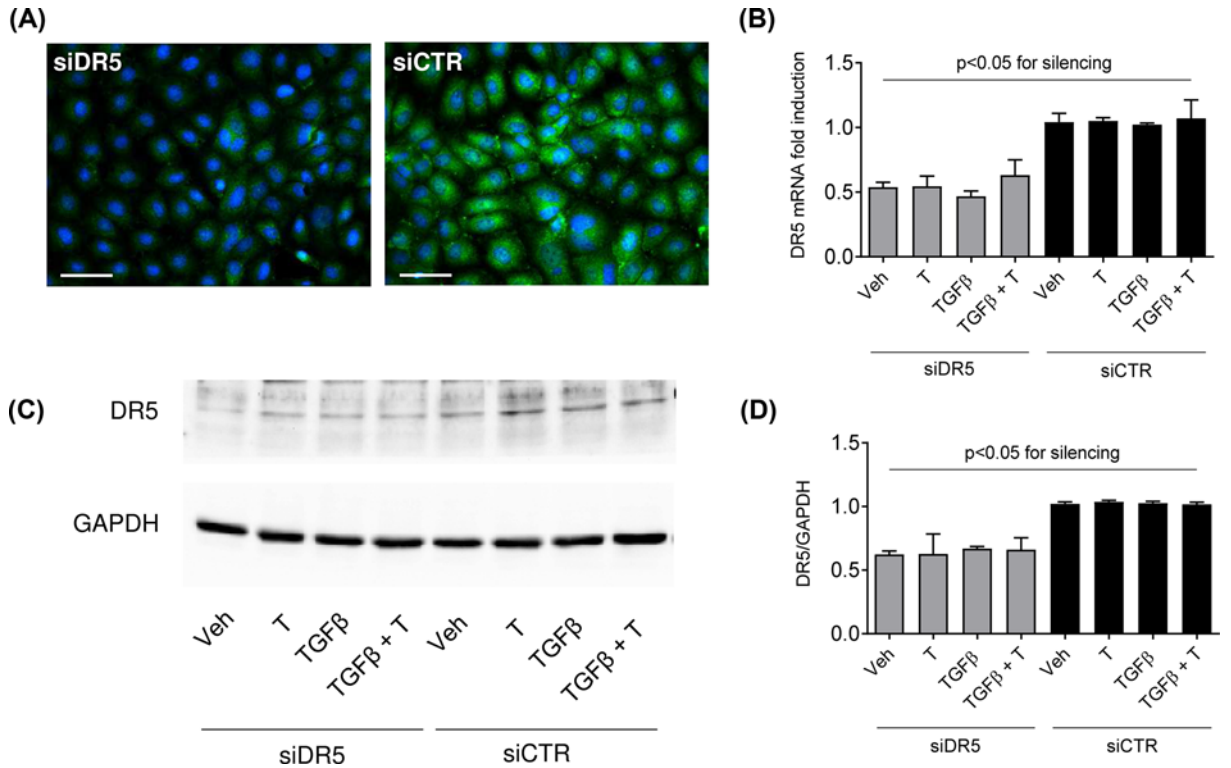

Figure 5. *Dr5* silencing

(**A**) Representative immunofluorescence stainings of DR5 with and without *Dr5* silencing (siDR5 and siCTR, respectively). (**B**) *Dr5* gene expression reported as mRNA fold induction normalized to the mRNA level of siCTR + Veh. (**C**,**D**) Representative blot and densitometric analysis of DR5 in NRK-52E cells with and without *Dr5* silencing (siDR5 and siCTR, respectively). Data are normalized to GAPDH. Results were obtained by three independent experiments and are presented as mean ± SEM. Two-way ANOVA showed $P<0.05$ for silencing. Veh is for vehicle, T is for TRAIL. Scale bar represents 100 μm.

of db/db mice we found a significant increase in p62, which was significantly reduced by TRAIL treatment (Figure 8A,B). A similar trend was observed in TGF-β1-treated cells (Figure 8C,D).

Discussion

During the last decade, TRAIL has attracted attention not only for its therapeutic effect as an anti-cancer agent, but also as a potential treatment for diabetes and its associated diseases [21]. In particular, *in vivo* studies have shown that TRAIL delivery ameliorated type 1 [7] and type 2 diabetes [8,9], while TRAIL deficiency was associated with worsening of glucose control [6,10]. In this scenario, this is the first study evaluating TRAIL effects on an animal model of severe type 2 diabetes complicated with nephropathy.

With respect to diabetes and glucose control, in the present study, TRAIL treatment did not modify food intake, body weight, hyperinsulinemia and hyperglycemia. These results differ from our previous reports where we showed that TRAIL treatment significantly reduced the metabolic abnormalities induced by a high-fat diet [8,9], with reduction in liver steatosis [9,22] and body fat mass and improvement of skeletal muscle fat oxidation [8]. However, it has to be taken into account that in the present study, TRAIL effects were tested in a genetic model of type 2 diabetes, whose metabolic phenotype is extreme as compared with the one induced by a high-fat diet. In particular, the phenotype of db/db mice is due to the lack of the full-length Ob-Rb receptor, which leads to unresponsiveness to leptin in the hypothalamus and elevate leptin concentration, unlimited food appetite, morbid obesity and diabetes.

As expected, male db/db mice exhibited hyperleptinemia, which was only slightly reduced by TRAIL. By contrast, TRAIL was able to significantly reduce circulating IL-6 and resistin. These data are consistent with previous observations that TRAIL has anti-inflammatory actions [8,9]. Nevertheless, the reduction in IL-6 and resistin might point to additional (indirect) mechanisms of TRAIL actions, such as an amelioration of kidney function, as suggested by

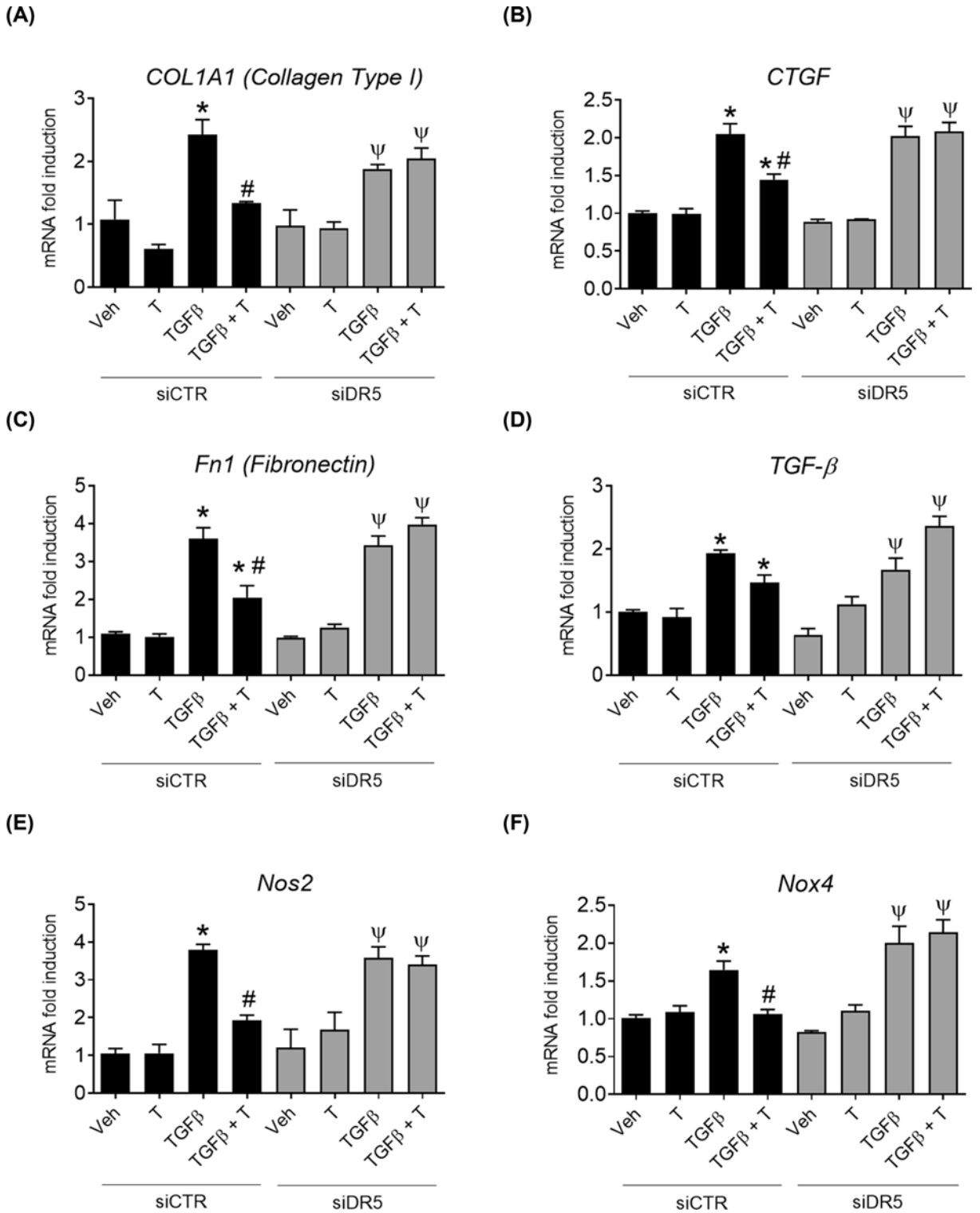

Figure 6. Effects of TRAIL treatment on tubular cell gene expression

The gene expression of *Col1a1* (**A**)*, CTGF* (**B**)*, Fn1 (fibronectin*) (**C**), *TGF-*β (**D**)*, Nos2* (*iNos)* (**E**) and *Nox4* (**F**) were reported as mRNA fold induction normalized to the mRNA level of siCTR + Veh. Results were obtained by three independent experiments and are presented as mean ± SEM. $^{*}P<0.05$ vs Veh and $^{\#}P<0.05$ vs TGFβ in the siCTR group; $^{\Psi}P<0.05$ vs Veh in the siDR5 group. Veh is for vehicle, T is for TRAIL.

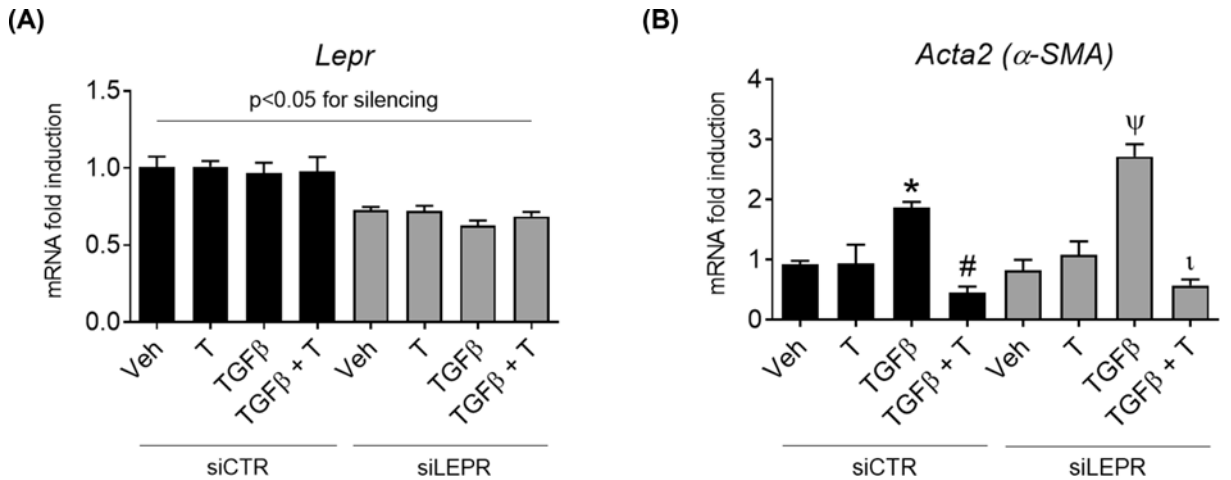

Figure 7. Silencing of Leptin receptor (*Lepr*) does not affect TRAIL anti-fibrotic effects

(**A**) *Lepr*, (**B**) *Acta2* (α-*SMA*) gene expression reported as mRNA fold induction normalized to the mRNA level of siCTR + Vehicle. Results were obtained by three independent experiments and are presented as mean ± SEM. **P*<0.05 vs Veh and $^{\#}P$<0.05 vs TGFβ in the siCTR group; $^{\Psi}P$<0.05 vs Veh and $^{\iota}P$<0.05 vs TGF-β in the siLEPR group.

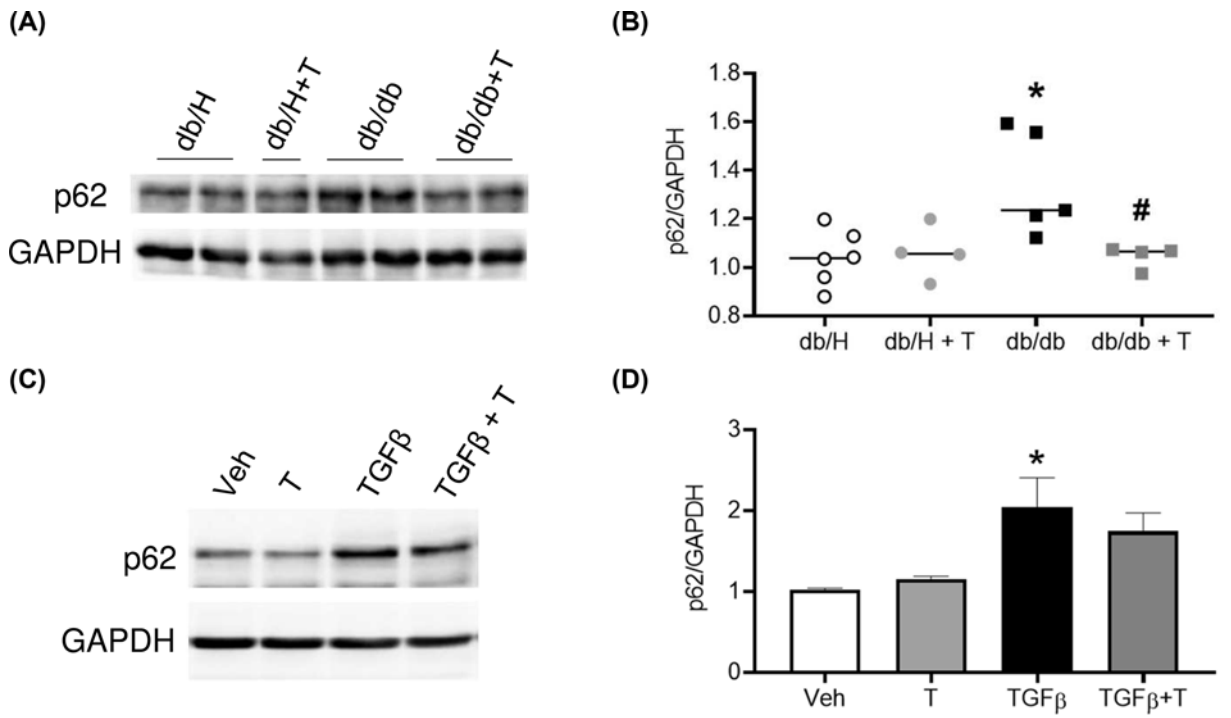

Figure 8. TRAIL reduces p62 levels in the kidneys of db/db mice

(**A**,**B**) Representative blot and densitometric analysis of p62 in the kidneys of db/H and db/db mice with and without TRAIL treatment. **P*=0.017 vs db/H and $^{\#}P$=0.016 vs db/db, Mann–Whitney test. (**C**,**D**) Representative blot and densitometric analysis of NRK-52E cells with TGF-β1 alone and in combination with TRAIL. Results were obtained by three independent experiments and are presented as mean ± SEM. Veh is for vehicle, T is for TRAIL.

the reduction in creatinine levels. It has been demonstrated that both IL-6 and resistin are inversely related to renal function [23,24].

The db/db mouse is one of the models that are appropriate for the study of diabetic nephropathy, as they develop glomerular hypertrophy, mesangial matrix expansion and albuminuria [12,14,25]. In the present study, we found that

TRAIL treatment significantly ameliorated the morphological changes of diabetic nephropathy as it reduced glomerular hypertrophy and glomerulosclerosis, and in the tubulum-interstitium it significantly reduced tubular hypertrophy and the area of interstitial inflammatory infiltrates. In addition, in the kidney, TRAIL significantly reduced vimentin expression, while in the glomeruli, it significantly reduced the glomerular expression of collagen IV and nitrotyrosine, which are markers of fibrosis and oxidative stress, while the expression of synaptopodin which is a podocyte marker, increased in the db/db mice treated with TRAIL as compared with the db/db mice. Also the gene expression analysis showed that TRAIL significantly down-regulated several profibrotic genes, such as *Col1a1*, *Fibronectin* and *Vimentin,* as well as proinflammatory genes such as *IL-1*β and *IL-6*, whose gene expression was significantly increased in db/db mice. These results indicate that TRAIL has significant anti-fibrotic actions and are consistent with the data reported by Cartland et al. [26], who found that TRAIL deficiency worsened diabetic nephropathy. In particular, TRAIL/ApoE-knockout mice fed a high-fat diet for 20 weeks displayed more glomerular matrix accumulation, as assessed by PAS and vimentin staining, and more glomerular fibrosis, as assessed by collagen IV staining. These changes were associated with a significant increase in albuminuria.

By contrast, in our study, TRAIL protective effects were not associated with a significant reduction in albuminuria. It has to be noted that our data did not show any constitutive reason as to why the db/db mouse should not respond to TRAIL treatment. When we looked at the renal expression of DR5, which is TRAIL-specific receptor, this was unchanged in the glomeruli and tubuli of db/db mice. Second, when we silenced the leptin receptor, we did not find a difference in the cell response to TRAIL, indicating that the deletion mutation of leptin should not impair TRAIL signaling in the db/db mouse. Interestingly, the discrepancy that we found between the morphological improvements induced by TRAIL and albuminuria unresponsiveness are consistent with the data of other Authors, who reported that even the administration of an anti-TGFβ antibody did not attenuate the degree of albuminuria in the db/db mouse despite its beneficial effects on glomerular matrix expansion and creatinine levels [27].

A possible reason for TRAIL not lowering albuminuria, is that TRAIL did not have metabolic effects and did not lower glucose and leptin. Beside hyperglycemia and insulin resistance, also hyperleptinemia might promote kidney damage. This is supported by the observation that, although both ob/ob and db/db share an impairment of leptin signaling, ob/ob mice, which are leptin-deficient rarely develop renal disease, while db/db mice that are hyperleptinemic usually develop diabetic nephropathy [28]. Several studies have found a direct correlation between leptin and proteinuria [29–31]. The possibility that leptin had direct actions against the kidney was shown by Han et al. demonstrating that, even though db/db mice do not express the full-length leptin receptor, they exhibit the short Ob-Ra isoform in many tissues, which can mediate local actions that seem to differ from those of the long isoform activation [28]. In particular, in these experiments, leptin stimulated collagen production in db/db mesangial cells [28].

In the present study, TRAIL anti-fibrotic actions were further confirmed by *in vitro* experiments, where we found that TRAIL significantly ameliorated the morphological changes induced by TGF-β1, as it significantly reduced the EMT in epithelial tubular cells, by binding to its specific receptor DR5. This was associated with similar changes in the expression of *Col1a1, CTGF, fibronectin*, *TGF-β,* as well as *iNos* and *Nox4,* which increased after TGF-β1 stimulation and were reduced by TRAIL cotreatment. Many studies have described an increased expression and activation of TGF-β in progressive forms of human kidney disease [32]. In particular, TGF-β signaling has been implicated in myofibroblasts recruitment, which are considered the dominant collagen-producing cells in many pathologies including kidney fibrosis, and which derive through differentiation not only from EMT but also from bone marrow and endothelial-to-mesenchymal transition [33].

Although TRAIL is an inducer of apoptosis, in our study it did not affect cell viability, possibly due to the dose that was used, which was lower than the dose-inducing apoptosis in other studies [34]. In the kidney, we did not see an effect on BAX/Bcl2 ratio. By contrast, in db/db mice, TRAIL increased the expression of *ATG5*, which is an autophagy-related gene, suggesting a possible up-regulation of autophagy. Authophagy is a degradation system that regulates intracellular homeostasis. Animal models lacking autophagy-related genes have demonstrated that autophagy is implicated in the development of kidney disease due to an impaired removal of damaged proteins, and production of cytokines and autoantibodies. Interestingly, it has been demonstrated that TRAIL signaling can lead either to apoptosis or to autophagy [35]. Consistent with this concept, in the present study we found that TRAIL treatment was able to reduce the levels of p62 in db/db mice. p62 is a substrate for authophagy degradation, which decreases during autophagy progression, whereas it increases with the inhibition of autophagy. Therefore, a possible mechanism underlying TRAIL anti-fibrotic actions is that TRAIL might promote autophagy in type 2 diabetes, where it is generally reduced [20].

In conclusion, in a mouse model of severe type 2 diabetes and diabetic nephropathy, TRAIL treatment significantly ameliorated glomerular morphological changes and this was associated with a significant reduction in the EMT induced by TGF-β1. These data confirm TRAIL protective effect against organ/kidney damage and shed light on to its

promising anti-fibrotic actions, which are independent of glucose control. TRAIL anti-fibrotic actions might be due to the rescue of autophagy in diabetes.

Clinical perspectives

- TRAIL has attracted attention not only for its therapeutic effects as an anti-cancer agent, but also as a potential treatment for diabetes. It is currently unknown whether TRAIL-positive effects are maintained in more severe forms of type 2 diabetes, and whether they include renoprotection.
- Our study shows that in the db/db mouse, which is a mouse model of diabetic nephropathy, TRAIL treatment significantly ameliorated glomerular morphological changes and this was associated with a significant reduction in the EMT induced by TGF-β1 *in vitro*. In the db/db mouse, creatinine, as well as circulating IL-6 and resistin were significantly lowered by TRAIL treatment. Proteinuria did not change—possibly due to the fact that TRAIL did not have metabolic effects.
- These data confirm TRAIL protective effects against organ damage and shed light on to promising anti-fibrotic actions, which are independent of glucose control and might rely on the promotion of autophagy.

Competing Interests

The authors declare that there are no competing interests associated with the manuscript.

Funding

This work was supported by the Italian Ministry of Health [grant number GR-2013-02357830 (to S.B.)]; and the Università degli Studi di Trieste [grant number FRA 2016 (to B.F.)].

Author Contribution

B.T. was responsible for acquisition, analysis and interpretation of *in vivo* data and manuscript preparation. F.T. was responsible for acquisition, analysis and interpretation of *in vitro* data and manuscript preparation. V.T. was responsible for TRAIL preparation and interpretation of data. A.M. was responsible for acquisition and analysis of *in vivo* data. G.Z., P.S. and B.F. were responsible for conception, interpretation of data and article revision for important intellectual content. S.B. was responsible for conception and design, acquisition, analysis and interpretation of data, and drafting the article. All the authors have read and approved the submission of this manuscript.

Abbreviations

ACR, albumin/creatinine ratio; DR5, death receptor 5; EMT, epithelial-to-mesenchymal transition; H/E, Hematoxylin and Eosin; IL, interleukin; IPGTT, intraperitoneal glucose tolerance test; IPITT, intraperitonal insulin tolerance test; LEPR, leptin receptor; MCP, monocyte chemoattractant protein; MTT assay, tetrazolium bromide dye reaction assay; PAS, Periodic acid–Schiff; SMA, smooth muscle actin; SQSTM1, sequestosome-1 (p62); TRAIL, TNF-related apoptosis-inducing ligand.

References

1 Wiley, S.R., Schooley, K., Smolak, P.J., Din, W.S., Huang, C.P., Nicholl, J.K. et al. (1995) Identification and characterization of a new member of the TNF family that induces apoptosis. *Immunity* **3**, 673–682, https://doi.org/10.1016/1074-7613(95)90057-8

2 Pitti, R.M., Marsters, S.A., Ruppert, S., Donahue, C.J., Moore, A. and Ashkenazi, A. (1996) Induction of apoptosis by Apo-2 ligand, a new member of the tumor necrosis factor cytokine family. *J. Biol. Chem.* **271**, 12687–12690, https://doi.org/10.1074/jbc.271.22.12687

3 Ashkenazi, A., Pai, R.C., Fong, S., Leung, S., Lawrence, D.A., Marsters, S.A. et al. (1999) Safety and antitumor activity of recombinant soluble Apo2 ligand. *J. Clin. Invest.* **104**, 155–162, https://doi.org/10.1172/JCI6926

4 Bernardi, S., Secchiero, P. and Zauli, G. (2012) State of art and recent developments of anti-cancer strategies based on TRAIL. *Recent Pat. Anticancer Drug Discov.* **7**, 207–217, https://doi.org/10.2174/157489212799972927

5 Lamhamedi-Cherradi, S.E., Zheng, S., Tisch, R.M. and Chen, Y.H. (2003) Critical roles of tumor necrosis factor-related apoptosis-inducing ligand in type 1 diabetes. *Diabetes* **52**, 2274–2278, https://doi.org/10.2337/diabetes.52.9.2274

6 Mi, Q.S., Ly, D., Lamhamedi-Cherradi, S.E., Salojin, K.V., Zhou, L., Grattan, M. et al. (2003) Blockade of tumor necrosis factor-related apoptosis-inducing ligand exacerbates type 1 diabetes in NOD mice. *Diabetes* **52**, 1967–1975, https://doi.org/10.2337/diabetes.52.8.1967

7 Zauli, G., Toffoli, B., di Iasio, M.G., Celeghini, C., Fabris, B. and Secchiero, P. (2010) Treatment with recombinant tumor necrosis factor-related apoptosis-inducing ligand alleviates the severity of streptozotocin-induced diabetes. *Diabetes* **59**, 1261–1265, https://doi.org/10.2337/db09-1771

8 Bernardi, S., Zauli, G., Tikellis, C., Candido, R., Fabris, B., Secchiero, P. et al. (2012) TNF-related apoptosis-inducing ligand significantly attenuates metabolic abnormalities in high-fat-fed mice reducing adiposity and systemic inflammation. *Clin. Sci. (Lond.)* **123**, 547–555, https://doi.org/10.1042/CS20120176

9 Bernardi, S., Toffoli, B., Tisato, V., Bossi, F., Biffi, S., Lorenzon, A. et al. (2018) TRAIL reduces impaired glucose tolerance and NAFLD in the high-fat diet fed mouse. *Clin. Sci. (Lond.)* **132**, 69–83, https://doi.org/10.1042/CS20171221

10 Di Bartolo, B.A., Chan, J., Bennett, M.R., Cartland, S., Bao, S., Tuch, B.E. et al. (2011) TNF-related apoptosis-inducing ligand (TRAIL) protects against diabetes and atherosclerosis in Apoe (-)/(-) mice. *Diabetologia* **54**, 3157–3167, https://doi.org/10.1007/s00125-011-2308-0

11 Bernardi, S., Voltan, R., Rimondi, E., Melloni, E., Milani, D., Cervellati, C. et al. (2019) TRAIL, OPG, and TWEAK in kidney disease: biomarkers or therapeutic targets? *Clin. Sci. (Lond.)* **133**, 1145–1166, https://doi.org/10.1042/CS20181116

12 Forbes, J.M. and Cooper, M.E. (2013) Mechanisms of diabetic complications. *Physiol. Rev.* **93**, 137–188, https://doi.org/10.1152/physrev.00045.2011

13 Chen, H., Charlat, O., Tartaglia, L.A., Woolf, E.A., Weng, X., Ellis, S.J. et al. (1996) Evidence that the diabetes gene encodes the leptin receptor: identification of a mutation in the leptin receptor gene in db/db mice. *Cell* **84**, 491–495, https://doi.org/10.1016/S0092-8674(00)81294-5

14 Sharma, K., McCue, P. and Dunn, S.R. (2003) Diabetic kidney disease in the db/db mouse. *Am. J. Physiol. Renal Physiol.* **284**, F1138–F1144, https://doi.org/10.1152/ajprenal.00315.2002

15 MacFarlane, M., Ahmad, M., Srinivasula, S.M., Fernandes-Alnemri, T., Cohen, G.M. and Alnemri, E.S. (1997) Identification and molecular cloning of two novel receptors for the cytotoxic ligand TRAIL. *J. Biol. Chem.* **272**, 25417–25420, https://doi.org/10.1074/jbc.272.41.25417

16 Shih, I.M., Torrance, C., Sokoll, L.J., Chan, D.W., Kinzler, K.W. and Vogelstein, B. (2000) Assessing tumors in living animals through measurement of urinary beta-human chorionic gonadotropin. *Nat. Med.* **6**, 711–714, https://doi.org/10.1038/76299

17 Burns, W.C., Twigg, S.M., Forbes, J.M., Pete, J., Tikellis, C., Thallas-Bonke, V. et al. (2006) Connective tissue growth factor plays an important role in advanced glycation end product-induced tubular epithelial-to-mesenchymal transition: implications for diabetic renal disease. *J. Am. Soc. Nephrol.* **17**, 2484–2494, https://doi.org/10.1681/ASN.2006050525

18 Toffoli, B., Zennaro, C., Winkler, C., Giordano Attianese, G.M.P., Bernardi, S., Carraro, M. et al. (2018) Hemicentin 1 influences podocyte dynamic changes in glomerular diseases. *Am. J. Physiol. Renal Physiol.* **314**, F1154–F1165, https://doi.org/10.1152/ajprenal.00198.2017

19 Bernardi, S., Toffoli, B., Zennaro, C., Tikellis, C., Monticone, S., Losurdo, P. et al. (2012) High-salt diet increases glomerular ACE/ACE2 ratio leading to oxidative stress and kidney damage. *Nephrol. Dial. Transplant.* **27**, 1793–1800, https://doi.org/10.1093/ndt/gfr600

20 Sakai, S., Yamamoto, T., Takabatake, Y., Takahashi, A., Namba-Hamano, T., Minami, S. et al. (2019) Proximal tubule autophagy differs in Type 1 and 2 diabetes. *J. Am. Soc. Nephrol.* **30**, 929–945, https://doi.org/10.1681/ASN.2018100983

21 Harith, H.H., Morris, M.J. and Kavurma, M.M. (2013) On the TRAIL of obesity and diabetes. *Trends Endocrinol. Metab.* **24**, 578–587, https://doi.org/10.1016/j.tem.2013.07.001

22 Cartland, S.P., Harith, H.H., Genner, S.W., Dang, L., Cogger, V.C., Vellozzi, M. et al. (2017) Non-alcoholic fatty liver disease, vascular inflammation and insulin resistance are exacerbated by TRAIL deletion in mice. *Sci. Rep.* **7**, 1898, https://doi.org/10.1038/s41598-017-01721-4

23 Moreno, L.O., Salvemini, L., Mendonca, C., Copetti, M., De Bonis, C., De Cosmo, S. et al. (2015) Serum resistin and glomerular filtration rate in patients with type 2 diabetes. *PLoS ONE* **10**, e0119529, https://doi.org/10.1371/journal.pone.0119529

24 Hiramoto, J.S., Katz, R., Peralta, C.A., Ix, J.H., Fried, L., Cushman, M. et al. (2012) Inflammation and coagulation markers and kidney function decline: the Multi-Ethnic Study of Atherosclerosis (MESA). *Am. J. Kidney Dis.* **60**, 225–232, https://doi.org/10.1053/j.ajkd.2012.02.335

25 Kitada, M., Ogura, Y. and Koya, D. (2016) Rodent models of diabetic nephropathy: their utility and limitations. *Int. J. Nephrol. Renovasc. Dis.* **9**, 279–290, https://doi.org/10.2147/IJNRD.S103784

26 Cartland, S.P., Erlich, J.H. and Kavurma, M.M. (2014) TRAIL deficiency contributes to diabetic nephropathy in fat-fed ApoE-/- mice. *PLoS ONE* **9**, e92952, https://doi.org/10.1371/journal.pone.0092952

27 Ziyadeh, F.N., Hoffman, B.B., Han, D.C., Iglesias-De La Cruz, M.C., Hong, S.W., Isono, M. et al. (2000) Long-term prevention of renal insufficiency, excess matrix gene expression, and glomerular mesangial matrix expansion by treatment with monoclonal antitransforming growth factor-beta antibody in db/db diabetic mice. *Proc. Natl. Acad. Sci. U.S.A.* **97**, 8015–8020, https://doi.org/10.1073/pnas.120055097

28 Han, D.C., Isono, M., Chen, S., Casaretto, A., Hong, S.W., Wolf, G. et al. (2001) Leptin stimulates type I collagen production in db/db mesangial cells: glucose uptake and TGF-beta type II receptor expression. *Kidney Int.* **59**, 1315–1323, https://doi.org/10.1046/j.1523-1755.2001.0590041315.x

29 Rudberg, S. and Persson, B. (1998) Serum leptin levels in young females with insulin-dependent diabetes and the relationship to hyperandrogenicity and microalbuminuria. *Horm. Res.* **50**, 297–302, https://doi.org/10.1159/000023294

30 Wilson, C., Nelson, R., Nicolson, M. and Pratley, R. (1998) Plasma leptin concentrations: no difference between diabetic Pima Indians with and without nephropathy. *Diabetologia* **41**, 861–862

31 Fruehwald-Schultes, B., Kern, W., Beyer, J., Forst, T., Pfutzner, A. and Peters, A. (1999) Elevated serum leptin concentrations in type 2 diabetic patients with microalbuminuria and macroalbuminuria. *Metabolism* **48**, 1290–1293, https://doi.org/10.1016/S0026-0495(99)90270-6

32 Meng, X.M., Nikolic-Paterson, D.J. and Lan, H.Y. (2016) TGF-beta: the master regulator of fibrosis. *Nat. Rev. Nephrol.* **12**, 325–338, https://doi.org/10.1038/nrneph.2016.48

33 LeBleu, V.S., Taduri, G., O'Connell, J., Teng, Y., Cooke, V.G., Woda, C. et al. (2013) Origin and function of myofibroblasts in kidney fibrosis. *Nat. Med.* **19**, 1047–1053, https://doi.org/10.1038/nm.3218

34 Lu, M., Marsters, S., Ye, X., Luis, E., Gonzalez, L. and Ashkenazi, A. (2014) E-cadherin couples death receptors to the cytoskeleton to regulate apoptosis. *Mol. Cell* **54**, 987–998, https://doi.org/10.1016/j.molcel.2014.04.029

35 Nikoletopoulou, V., Markaki, M., Palikaras, K. and Tavernarakis, N. (2013) Crosstalk between apoptosis, necrosis and autophagy. *Biochim. Biophys. Acta* **1833**, 3448–3459, https://doi.org/10.1016/j.bbamcr.2013.06.001